Supplementary Information

Integrative analysis of fitness and metabolic effects of plasmids in *Pseudomonas aeruginosa* PAO1

Alvaro San Millan[1,2,Ψ,*], Macarena Toll-Riera[1,3,4,Ψ,*], Qin Qi[1], Alex Betts[1], Richard J Hopkinson[5,6], James McCullagh[5], R Craig MacLean[1].

[1] Department of Zoology, University of Oxford, OX2 6GG, Oxford, United Kingdom.

[2] Department of Microbiology, Hospital Universitario Ramon y Cajal (IRYCIS) and Network Research Centre for Epidemiology and Public Health (CIBERESP), 28034, Madrid, Spain.

[3] Department of Evolutionary Biology and Environmental Studies, University of Zurich, Zurich CH-8057, Switzerland.

[4] Swiss Institute of Bioinformatics, Quartier Sorge-Bâtiment Génopode, Lausanne 1015, Switzerland.

[5] Chemistry Research Laboratory, University of Oxford, OX1 3TA, Oxford, United Kingdom.

[6] Department of Chemistry, University of Leicester, LE1 7RH, Leicester, United Kingdom.

* These authors contributed equally to this work

[Ψ] Correspondence:

Alvaro San Millan: Department of Microbiology, Hospital Universitario Ramon y Cajal. Ctra. Colmenar Viejo Km 9,100. 28034, Madrid, Spain.

Email: alvsanmillan@gmail.com. Phone: +34636737538

Macarena Toll-Riera: Department of Evolutionary Biology and Environmental Studies, University of Zurich, Zurich, CH-8057, Switzerland.

Email: mtollriera@gmail.com. Phone: +41786981582

Supplementary Material and Methods

Bacterial strains, plasmids and culture conditions

The plasmids used in this study are described in Table 1. *P. aeruginosa* PAO1 was used as recipient strain. To measure plasmid-mediated activation of the SOS response, we used the reporter strain PAO1 WTp*lex*:lux, which was previously constructed in our laboratory (Torres-Barcelo et al 2015). To measure plasmid-mediated activation of QS system, we used the reporter PAO1 P*lasB*::lux (Popat et al 2012). Bacterial strains were cultured in LB broth at 37°C with continuous shaking (225 rpm) and on LB agar plates at 37°C (Fisher Scientific, NJ, USA). PAO1, WTp*lex*:lux and P*lasB*::lux were transformed by electroporation with the different plasmids as previously described (Choi and Schweizer 2006), using a Gene Pulser apparatus (Bio-Rad). Transformants were selected on LB agar plates containing antibiotics as previously described (San Millan et al 2014a, San Millan et al 2014b).

Competitive fitness assays

The fitness of each plasmid-carrying PAO1 clone was determined relative to a PAO1-GFP plasmid-free control strain. The GFP label did not produce a significant reduction in fitness in PAO1 (San Millan et al 2014b). Pre-cultures of the strains were incubated at 37°C with 225 rpm shaking overnight in 3 mL of LB broth. Pre-cultures were diluted 20-fold in 200 µL of fresh LB and incubated in the same conditions in 96-well plates until they reached mid-exponential phase (OD_{600} ≈ 0.5). Cultures of the strains were then mixed at a ratio of approximately 50% clone under study to 50% PAO1-GFP. The exact initial proportions were confirmed via flow cytometry using an Accuri C6 Flow Cytometer Instrument (BD Accuri, San Jose, CA, USA) with the following parameters: flow rate: 66 µL min^{-1}, core size: 22 µm, events recorded per sample: 10,000. Mixtures were diluted 400-fold in 200 µL of fresh LB and competed

in 96-well plates for 16 hours at 37°C with 225 rpm shaking (~8 generations). The final proportion was again measured by flow cytometry. The fitness of the strain carrying the plasmid(s) relative to the PAO1-GFP strain was determined using the formula (Lenski et al 1991):

$$W_{p+} = ln(Nfinal_{,p+}/Ninitial_{,p+})/ln(Nfinal_{,p-}/Ninitial_{,p-})$$

where W_{p+} is the relative fitness of the plasmid-bearing clone, $N_{initial,p+}$ and $N_{final,p+}$ are the numbers of cells of the plasmid-carrying clone before and after the competition, and $N_{initial,p-}$ and $N_{final,p-}$ are the numbers of PAO1-GFP cells before and after the competition. As a control, PAO1 and PAO1-GFP were competed in every experiment. We performed six biological replicates for each competition.

Growth curves in biolog EcoPlates

To assess bacterial growth in different environments, six biological replicates of PAO1 and three biological replicates of each of the six plasmid-carrying PAO1 clones were cultured in Biolog EcoPlates (Biolog, USA). Each clone was pre-cultured in 3 mL of LB overnight (37°C, 225 rpm), diluted down in M9 (1:1000 dilution), inoculated the EcoPlates and then cultured for 20 hours at 37°C. A Tecan Infinite M200 Pro plate reader was used to perform the growth curve experiments (Tecan Trading AG, Switzerland). Growth rates were estimated using the GrowthRates program (Hall et al 2014).

SOS induction assay

To assess plasmid-mediated SOS induction, luminescence production was measured over the growth curves of PAO1 WTp*lex*:lux (Torres-Barcelo et al 2015), the different plasmid-carrying WTp*lex*:lux strains, and a control strain with the plasmid-free WTp*lex*:lux growing in the presence of a sub-inhibitory concentration of the SOS-inducing antibiotic ciprofloxacin (45 µg/L). Each clone was pre-cultured in 3

mL of LB overnight (37°C, 225 rpm) and diluted in fresh LB (1:1000 dilution). Eight biological replicates were performed for each strain and the growth curves and luminescence production were measured using a BioTek Synergy H4 plate reader (BioTek Instruments, UK). The area under the curve of the light production over OD_{600} was measured during the exponential phase of the growth curves (first 7 hours) as a proxy for SOS induction (Figure 4).

Transcriptomics

RNA-Seq analysis was performed using the RNA samples from six strains: PAO1 wild-type, PAO1/pAMBL1, PAO1/pAMBL2, PAO1/pBS228, PAO1/pAKD1 and PAO1/RmS149. Samples were processed as previously described (San Millan et al 2015). RNA samples were obtained from two biological replicates (from three technical replicates each) per strain at mid-exponential phase of the growth curve (OD_{600} ≈ 0.4-0.5). Both library preparation (directional paired-end ribodepleted library) and sequencing (Illumina MiSeq) were performed at the Oxford Genomics Centre (Wellcome Trust Centre for Human Genetics at the University of Oxford).

RNA-Seq data were analysed using a pipeline that was developed in-house and previously described (San Millan et al 2015). Briefly, the raw reads were filtered using the NGS QC Toolkit (Patel and Jain 2012). Then, the filtered reads were mapped to our reference *P. aeruginosa* PAO1 genome (NC_002516.2 with the insertion of the phage RGP42 GQ141978.1) and to the reference sequence for the 5 plasmids (pAKD1: JN106164.1, RmS149: NC_007100.1, pBS228: NC_008357.1, PAMBL1: KP873172.1, pAMBL2: KP873171.1) using BWA (Li and Durbin 2010). On average, 48.9 x coverage was obtained; 98.7% of the bases had a Phred quality score of 20 or higher and 79.8% of the genes were covered by at least 5 reads. A PCA plot showed that the two biological replicates of each strain clustered together, discarding batch effects (Supplementary Figure S1). HTSeq was used to estimate gene counts

(Anders et al 2015), and DESeq2 (version 1.14.1) to perform differential gene expression analysis (Love et al 2014). The PAO1 clone used for these experiments is a laboratory-adapted clone with a mutation (insertion of an IS element) disrupting the promoter region of the quorum sensing (QS) modulator *lasR* gene. Therefore the genes under the control of LasR were excluded in the transcriptional analysis. To confirm the plasmids used in this study did not alter the expression of *P. aeruginosa* QS system, a PAO1 QS reporter strain was used, which contains a chromosomal *luxCDABE* cassette fusion to the promoter of the *lasB* gene, encoding the QS-dependent protease LasB (PAO1 P*lasB*::lux) (Popat et al 2012) (Supplementary Figure 7).

To compare within a given sample the expression of plasmid and chromosomal genes, TPM (transcript per million) was employed. FPKM (fragments per kilobase million) were computed using DESeq2 (Love et al 2014) and then transformed into TPM as follows:

$TPM_i = (FPKM_i / \Sigma_j FPKM_j) \times 10^6$

Functional enrichment analysis

The DAVID online tool was used to test for functional enrichment among the groups of differentially expressed genes (Huang da et al 2009). A given term was considered to be enriched when $P < 0.05$ after Benjamini correction.

Codon usage computation

Codon usage for coding sequences from each plasmid and *P. aeruginosa* PAO1 genome was computed using the *cusp* program inside the EMBOSS package (Rice et al 2000). The Codon Adaptation Index (CAI) was used to assess the similarity between the synonymous codon usage of a reference set of genes and that of the synonymous codon usage of plasmid genes. As a reference set, *P. aeruginosa* PAO1 genes coding for ribosomal proteins were used, as they are highly expressed,

and it is known that highly expressed genes have an optimized codon usage (Sharp and Li 1987). To compute the CAI, the CAIcal program was used (Puigbo et al 2008). To correct CAI values for gene expression, normalized TPM values were used; normalized TPM values were calculated by dividing each TPM value by the total number of TPMs of a given sample.

Biosynthetic cost

The biosynthetic cost of proteins (~P, activated phosphate) was computed by adding up, for each residue of the protein, the energy cost of each amino acid from precursors under respiratory conditions. Energy cost values were obtained from (Wagner 2005), and from (Akashi and Gojobori 2002), leading to very similar results. The biosynthetic costs were computed both for plasmids and *P. aeruginosa* PAO1 proteins. Correction for gene expression was carried out using the same approach used to correct CAI values.

Untargeted metabolomics

Samples for the metabolomic analysis were obtained from five biological replicates (prepared on five independent days) for each of the seven clones: PAO1 ancestral strain, PAO1/pAMBL1, PAO1/pAMBL2, PAO1/pBS228, PAO1/pAKD1, PAO1/RmS149 and PAO1/pNUK73. Each clone was pre-cultured in 3 mL of LB overnight (37°C, 225 rpm), diluted in 3 mL of fresh LB (1:30 dilution) and cultured in the same conditions as the day before until they reached an OD_{600} of approximately 0.5. 2 mL of these cultures were then centrifuged to form pellets (6000 rpm, 5 min.), washed in 1.5 mL of M9, and re-suspended in 5 mL of cold 80% methanol to ensure that the cells were dispersed in the methanol solution (and keeping the samples at -20°C). Each sample was then sonicated (40% amplitude, 100 cycles: 5'' on 10'' off), on ice to prevent overheating. 0.5 ml of each sample was then centrifuged at 14,800 rpm for 20 min. at 4°C; 200 µl of the supernatant was then transferred to a new tube

and stored at -80°C.

Each sample was analysed using ion exchange chromatography coupled to a Q-Exactive HF Hybrid Quadrupole-Orbitrap mass spectrometer. The ion chromatography system (ICS-5000+) incorporated an electrolytic anion generator (KOH), which was programmed to produce a OH^- gradient over 37 min. An inline electrolytic suppressor removed OH^- ions and cations from the post-column eluent stream prior to MS analysis (Thermo Scientific Dionex AERS 500). A 10 µL partial loop injection was used for all analyses and the chromatographic separation was performed using a Thermo Scientific Dionex IonPac AS11-HC 2 × 250 mm, 4 µm particle size column with a Dionex Ionpac AG11-HC 4 µm 2x50 guard column inline. The IC flow rate was 0.250 mL/min. The total run time was 37 mins and the hydroxide ion gradient comprised as follows: 0 mins, 0 mM; 1 min, 0 mM; 15 mins, 60 mM; 25 mins, 100 mM; 30 mins, 100 mM; 30.1 mins, 0 mM; 37 mins, 0 mM. Analysis was performed in negative ion mode using a scan-range from *m/z* 60-900 and resolution set to 70,000. The tune file source parameters were set as follows: Sheath gas flow 60 mL/min; Aux gas flow 20 mL/min; Spray voltage 3.6v; Capillary temperature 320°C; S-lens RF value 70; Heater temperature 350°C. AGC target was set to 1e6v ions and the Max IT value was 250 ms. The column temperature was kept at 30°C throughout the experiment. Full scan and MS/MS data were acquired in continuum mode. We used Progenesis QI (Waters, Elstree, UK) software for data processing. This included alignment of retention times, peak picking by identification of natural abundance isotope peaks, characterising multiple adducts forms and identification of metabolites using retention time and fragmentation patterns from authentic metabolite standards and matching accurate mass and isotope abundances experimentally determined with theoretical values. Identifications were accepted according to the following criteria: <5ppm differences between measured and theoretical mass (based on chemical formula), <30 seconds differences between

authentic standard and analyte retention times, isotope peak abundance measurements for analytes were >90% matched to the theoretical value generated from the chemical formula. Where measured, fragmentation patterns which were matched to a least the base peak and two additional peak matches in the MS/MS spectrum to within 6 ppm.

The results for each plasmid-carrying PAO1 combination were compared to the results from parental PAO1 to obtain the fold-change difference of metabolites due to plasmid carriage. For our analysis we used those metabolites, identified and non-identified, which were significant (q-value < 0.05) in at least one of the comparisons.

Statistical analyses

All statistical analyses and production of graphics were performed using R (R Core Team, 2014).

Data availability

The reads generated in this study have been deposited in the European Nucleotide Archive database with the accession number PRJEB24427 (http://www.ebi.ac.uk/ena/data/view/PRJEB24427).

Supplementary Figures

Supplementary Figure S1. PCA plot discarding batch effects in RNA-Seq replicates.

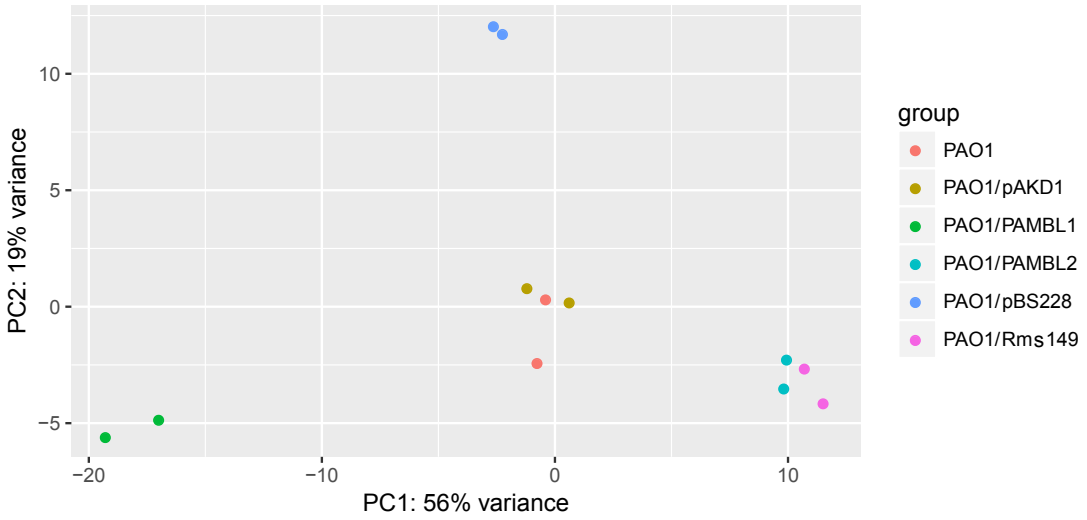

PCA plot from the RNA-Seq results using DESeq2 to check for batch effects. The two biological replicates from each strain grouped together, showing minimal batch effect.

Supplementary Figure S2. Direction of changes in expression of chromosomal genes of plasmid-carrying PAO1.

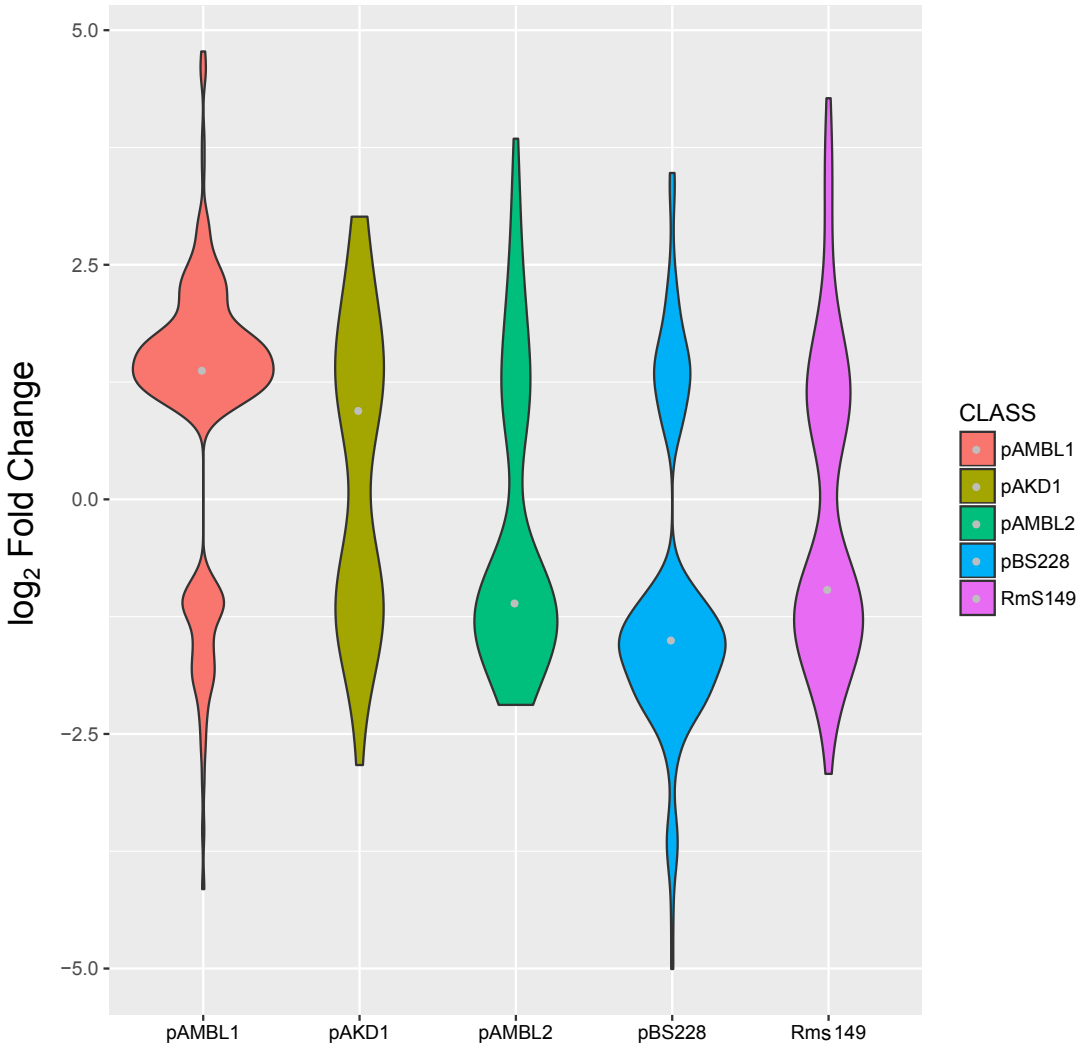

Violin plot representing the distribution of the fold changes in expression of chromosomal genes in the different plasmid-carrying PAO1 compared to plasmid-free PAO1. Only significant differentially expressed genes (DE) are represented in the figure (P-adjusted< 0.05). The grey dot represents the median value of the distribution. Costly plasmids (pAMBL2, pBS228 and Rms149) preferentially produced down-regulation of chromosomal genes (values of log2 fold change below 0), whereas beneficial plasmids (pAMBL1 and pAKD1) tended to entail up-regulation.

Supplementary Figure S3. Genes differentially expressed (DE) in common in the different plasmid-carrying PAO1.

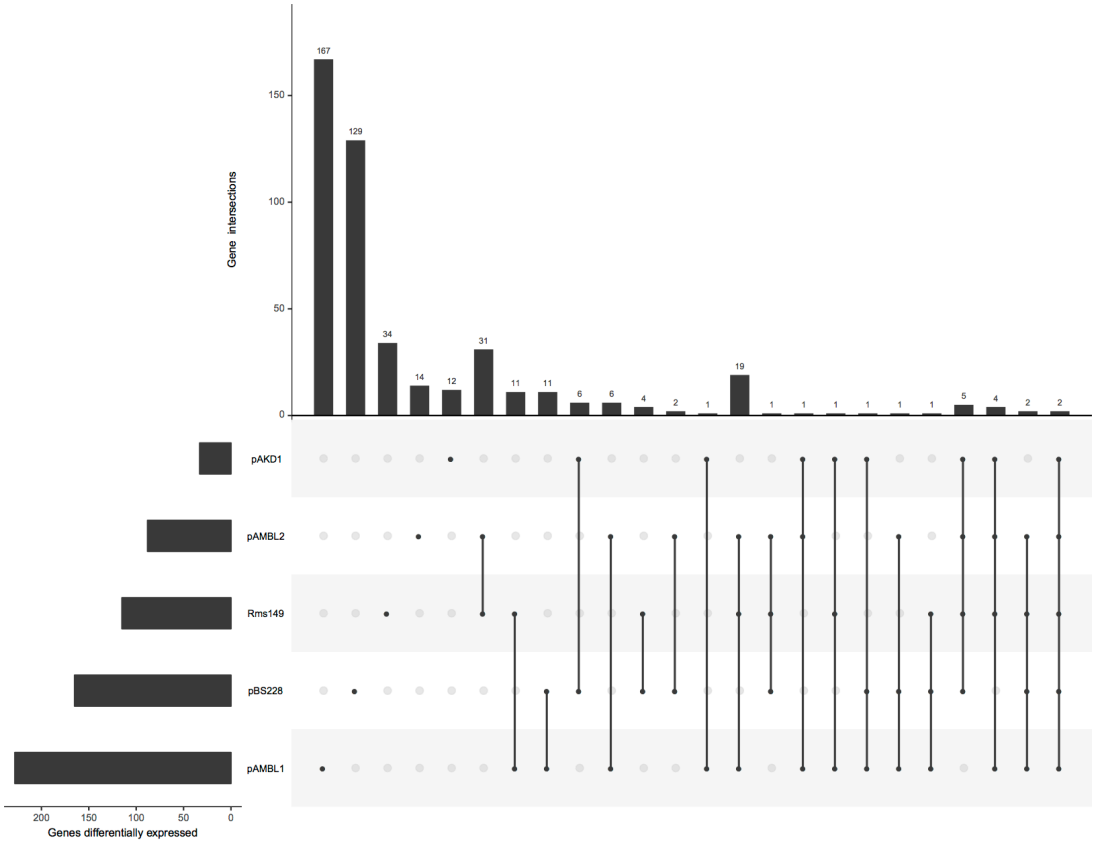

Diagram representing number of DE genes in each PAO1/plasmid combination, and shared DE genes between the different combinations. Note that each DE gene is only included in one category (bar), as in a Venn diagram.

Supplementary Figure S4. Distribution of codon adaptation index (CAI) values for chromosomal and plasmid genes.

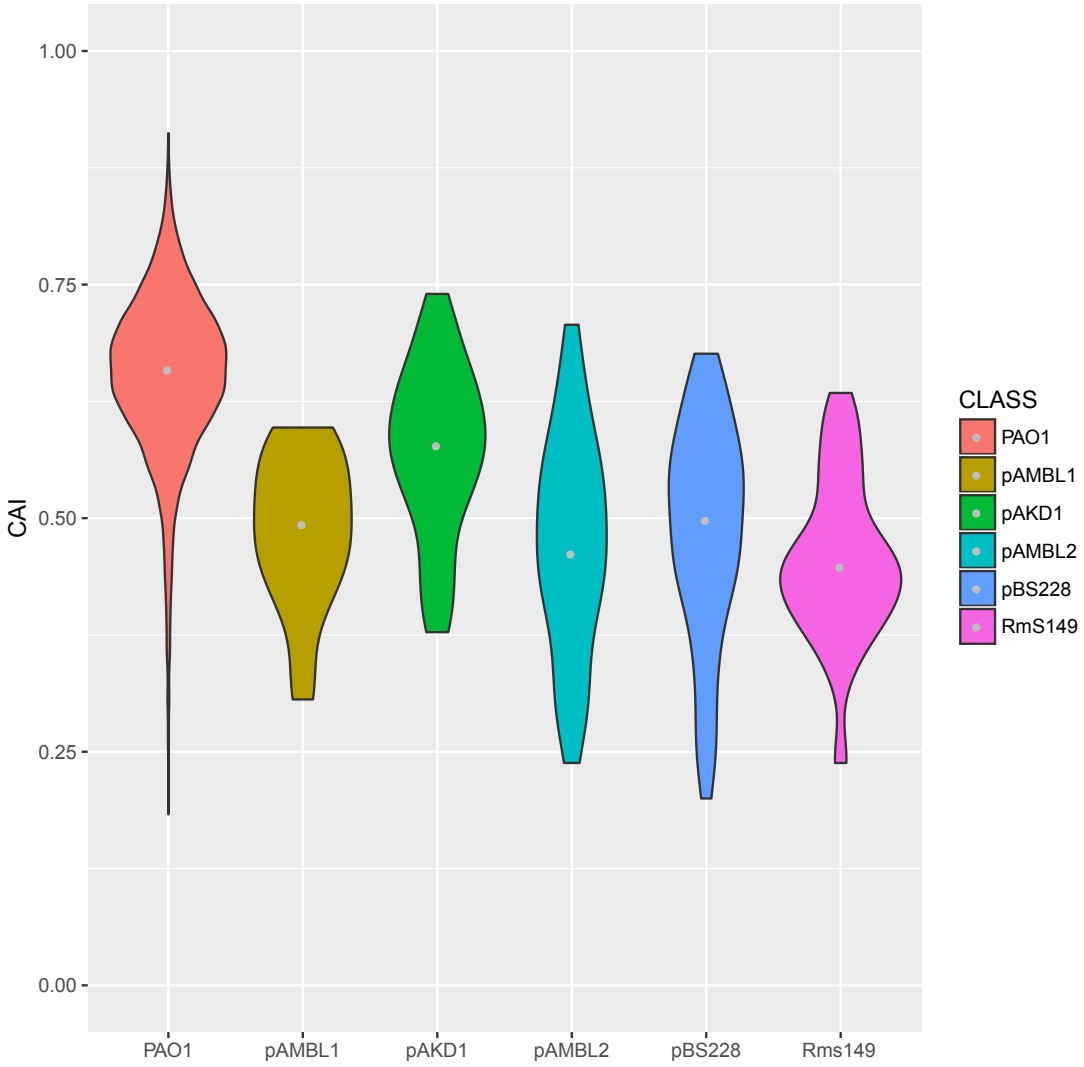

Violin plot representing the distribution of CAI values for all the genes in PAO1 chromosome (in red) and CAI values for the genes encoded in the different plasmids (see colour legend). The grey dot represents the median value of the distribution.

Supplementary Figure S5. Plasmids produce a parallel metabolic response in PAO1.

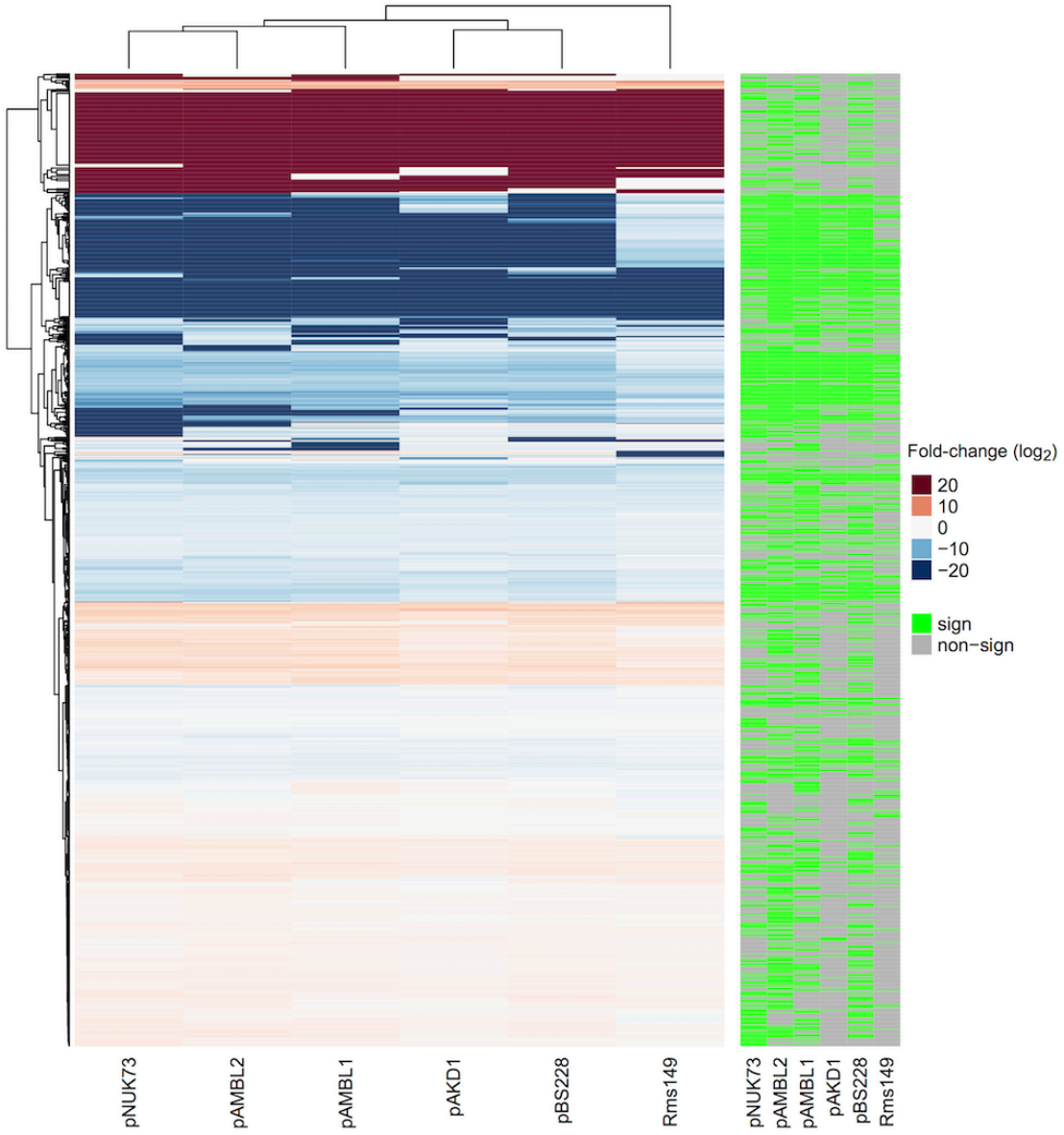

Different plasmids produce similar changes in metabolite abundance in the host bacterium *P. aeruginosa* PAO1. Heatmap representing those compounds with significant differences in abundance in at least one of the plasmid-carrying PAO1 compared to plasmid-free PAO1 (indicated by the green bars to the right of the figure). Compounds with higher abundance are represented in red, and compounds with lower abundance are represented in blue. The intensity of the colour is proportional to the differences in concentration, as indicated in the colour legend (log_2 fold-change). Compounds with an increase or decrease in abundance higher than 2^{20} fold are coloured at the same (maximum) intensity. We performed 5 replicates per strain for the metabolomic analysis.

Supplementary Figure S6. Correlation between plasmid GC content and relative fitness of the plasmid-bearing PAO1.

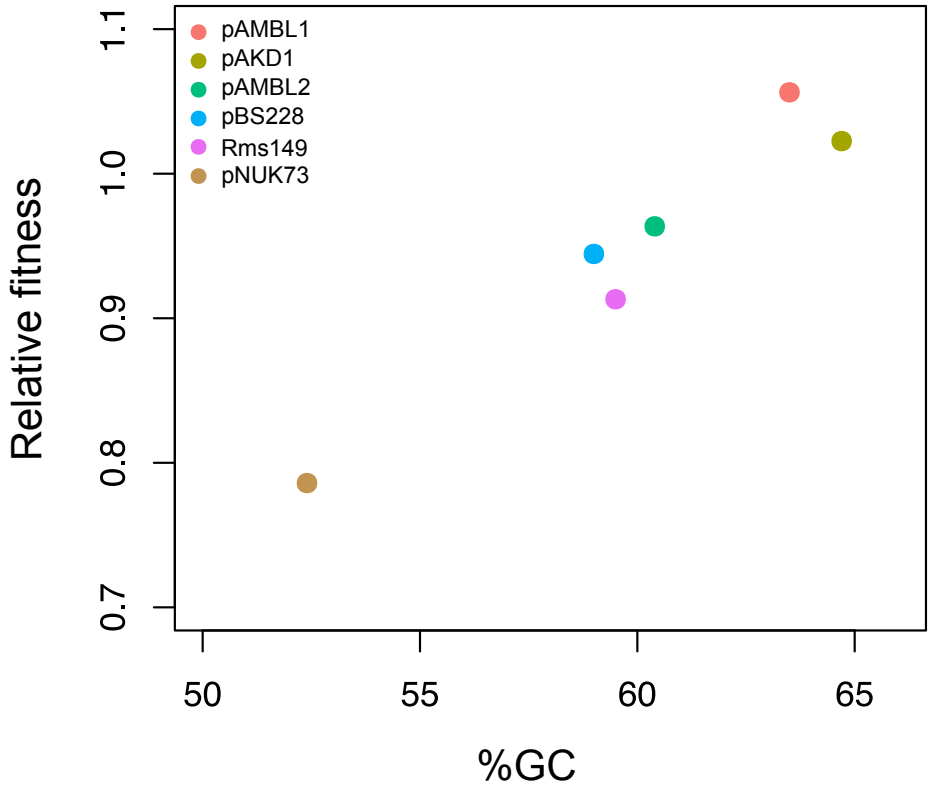

Plasmids with low GC content produce higher costs than plasmids with high GC content (more similar to the one from the host bacterial strain *P. aeruginosa* PAO1: 66.6%). There is a positive correlation between relative fitness of plasmid-carrying strain and the GC content of the plasmid (Pearson's test, r= 0.969, *P*= 0.001, t= 7.87, df= 4).

Supplementary Figure S7. Plasmids do not alter QS system in PAO1.

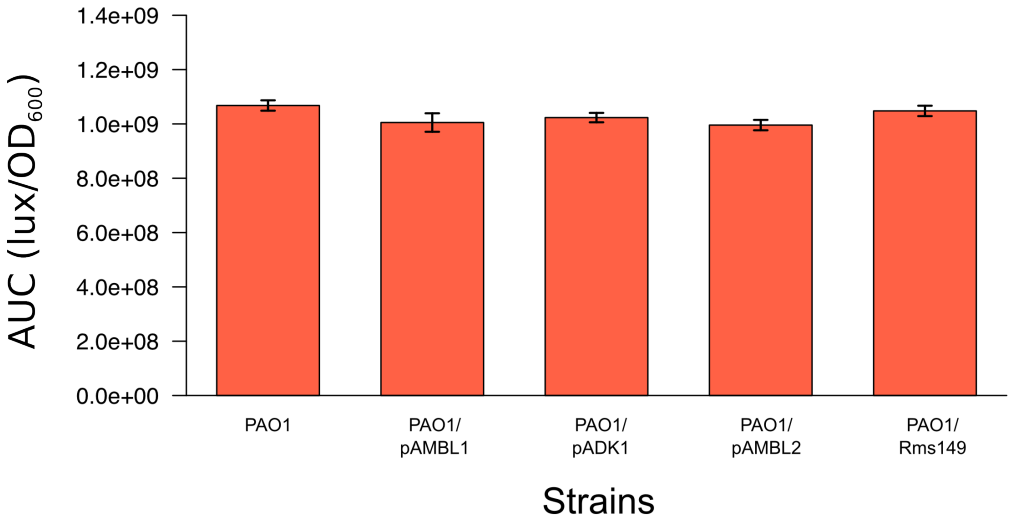

The plasmids in our collection do not affect the QS system in PAO1. The figure represents the area under the curve of luminescence production over OD600 [AUC (lux/OD600)] during the growth curves of PAO1 P*lasB*::lux reporter strain, which encodes a chromosomal *luxCDABE* fusion to the promoter of the *lasB* gene (P*lasB*) (PAO1 in the figure). We also present the AUC (lux/OD600) of the different plasmid-carrying P*lasB*::lux. We used pAKD1, pAMBL1, pAMBL2 and Rms149 plasmids (pBS228 has very poor electroporation efficiency due to its large size and we were not able to obtain a transformed strain). The bars indicate the average of 4 biological replicates (of six technical replicates each) and the error bars indicate the standard deviation.

Supplementary Tables

Supplementary Table S1. Transcriptional profiles of plasmids.

Levels of expression (in transcripts per million, TPM) of plasmid genes in the different plasmid-carrying PAO1.

Supplementary Table S2. Chromosomal genes DE due to presence of plasmids.

Table with the genes DE (under and over) for each of the 5 combinations of PAO1/plasmid compared to plasmid-free PAO1. The cut-off for classifying a gene as DE is padj <0.05.

Supplementary Table S3. Proportion of reads mapping to plasmids out of the total read counts in the cell.

Plasmid	Reads from plasmid (%)	Relative fitness of plasmid-carrying PAO1
pAMBL1	2.846	1.056
pAKD1	1.892	1.022
pAMBL2	1.745	0.963
pBS228	2.623	0.944
Rms149	1.927	0.913

Supplementary Table S4. Genes DE in common in plasmid-carrying PAO1.

Group of 38 genes DE in common in at least three of the five plasmid-carrying PAO1 analysed in this study. We also show the results from PAO1/pNUK73 from a previous analysis (San Millan et al 2015). Genes significantly DE are indicated with the value "1", and those showing no significant DE are indicated with "0". "+" indicates over-expression and "-" under-expression.

Supplementary Table S5. Functional enrichment analysis for DE genes.

Functional enrichment analysis of those genes DE in each plasmid-carrying PAO1 independently and in combination (all genes DE, under and over). The analysis is also shown for the genes DE in common in at least three plasmid-carrying PAO1 and for the groups of genes from the clusters in Figure 3.

Supplementary Table S6. CAI values for plasmids and PAO1 genes.

CAI and expression values for plasmid genes. CAI values for all PAO1 genes.

Supplementary Table S7. Expression of plasmid genes with different codon usages.

CAI	pAKD1	pAMBL1	pAMBL2	pBS228	Rms149
low	7.77%	79.40%	69.50%	32.51%	20.48%
medium	60.37%	20.60%	28.20%	56.27%	79.16%
high	31.86%	0	2.31%	11.22%	0.37%

Percentage of TPM for each plasmid that fall inside each CAI category. CAI categories were done using the mean CAI for plasmid genes (0.498) and adding or subtracting 1 standard deviation (0.110). For each CAI category, and each plasmid,

we summed the TPM of all the genes that fall in that specific CAI category, and we calculated the fraction that this represents from the total number of TPM for a given plasmid.

Supplementary Table S8. Biosynthetic cost of PAO1 and plasmids proteins.

Biosynthetic cost (measured in ~P, activated phosphate; energy costs were obtained from (Wagner 2005) and (Akashi and Gojobori 2002)) of the proteins encoded in PAO1 chromosome and in the different plasmids of the study. To correct for gene expression levels we weighted the biosynthetic cost by the expression levels (see methods).

Supplementary Table S9. Biosynthetic cost of proteins expressed from plasmids (relative to the total protein biosynthetic cost in the cell, corrected by expression).

Plasmid	Biosynthetic cost from plasmid (%)	Relative fitness of plasmid-carrying PAO1
pAMBL1	3.699	1.056
pAKD1	2.457	1.022
pAMBL2	3.724	0.963
pBS228	3.487	0.944
RmS149	2.512	0.913

Supplementary Table S10. Comparison of metabolite abundance between plasmid-carrying PAO1 and plasmid-free PAO1.

Metabolites presenting a significant difference (q-value<0.05) in abundance between the different plasmid-carrying PAO1 and the plasmid-free strain. Both identified and non-identified metabolites are presented.

Supplementary Table S11. Common metabolites with different abundance in plasmid-carrying PAO1.

Group of metabolites showing differences in abundance in common in plasmid-carrying PAO1 compared to plasmid-free PAO1. Both non-identified (first tab) and identified metabolites (second tab) are presented. Metabolites with different abundance are indicated with the value “1”, and those showing no significant difference are indicated with “0”.

Supplementary References

Akashi H, Gojobori T (2002). Metabolic efficiency and amino acid composition in the proteomes of Escherichia coli and Bacillus subtilis. *Proc Natl Acad Sci U S A* **99:** 3695-3700.

Anders S, Pyl PT, Huber W (2015). HTSeq-a Python framework to work with high-throughput sequencing data. *Bioinformatics* **31:** 166-169.

Choi KH, Schweizer HP (2006). mini-Tn7 insertion in bacteria with single attTn7 sites: example Pseudomonas aeruginosa. *Nat Protoc* **1:** 153-161.

Hall BG, Acar H, Nandipati A, Barlow M (2014). Growth Rates Made Easy. *Molecular Biology and Evolution* **31:** 232-238.

Huang da W, Sherman BT, Lempicki RA (2009). Systematic and integrative analysis of large gene lists using DAVID bioinformatics resources. *Nat Protoc* **4:** 44-57.

Lenski RE, Rose MR, Simpson SC, Tadler SC (1991). Long-Term Experimental Evolution in Escherichia coli. I. Adaptation and Divergence During 2,000 Generations. *The American Naturalist* **138:** 1315-1341.

Li H, Durbin R (2010). Fast and accurate long-read alignment with Burrows-Wheeler transform. *Bioinformatics* **26:** 589-595.

Love MI, Huber W, Anders S (2014). Moderated estimation of fold change and dispersion for RNA-seq data with DESeq2. *Genome Biol* **15:** 550.

Patel RK, Jain M (2012). NGS QC Toolkit: a toolkit for quality control of next generation sequencing data. *PLoS One* **7:** e30619.

Popat R, Crusz SA, Messina M, Williams P, West SA, Diggle SP (2012). Quorum-sensing and cheating in bacterial biofilms. *Proc Biol Sci* **279:** 4765-4771.

Puigbo P, Bravo IG, Garcia-Vallve S (2008). CAIcal: a combined set of tools to assess codon usage adaptation. *Biol Direct* **3:** 38.

Rice P, Longden I, Bleasby A (2000). EMBOSS: the European Molecular Biology Open Software Suite. *Trends Genet* **16:** 276-277.

San Millan A, Heilbron K, MacLean RC (2014a). Positive epistasis between co-infecting plasmids promotes plasmid survival in bacterial populations. *ISME J* **8:** 601-612.

San Millan A, Peña-Miller R, Toll-Riera M, Halbert ZV, McLean AR, Cooper BS *et al* (2014b). Positive selection and compensatory adaptation interact to stabilize non-transmissible plasmids. *Nat Commun* **5:** 5208.

San Millan A, Toll-Riera M, Qi Q, MacLean RC (2015). Interactions between horizontally acquired genes create a fitness cost in Pseudomonas aeruginosa. *Nat Commun* **6:** 6845.

Sharp PM, Li WH (1987). The codon Adaptation Index--a measure of directional synonymous codon usage bias, and its potential applications. *Nucleic Acids Res* **15:** 1281-1295.

Torres-Barcelo C, Kojadinovic M, Moxon R, MacLean RC (2015). The SOS response increases bacterial fitness, but not evolvability, under a sublethal dose of antibiotic. *Proc Biol Sci* **282:** 20150885.

Wagner A (2005). Energy constraints on the evolution of gene expression. *Mol Biol Evol* **22:** 1365-1374.